Mon. Not. R. Astron. Soc. **000**, 000–000 (0000) Printed 28 June 2011 (MN LATEX style file v2.2)

Effects of supermassive binary black holes on gravitational lenses

Nan Li [1⋆], Shude Mao[1,2]†, Liang Gao[1] and Avi Loeb+R. de Stefano ???[3]
[1]*National Astronomical Observatories, Chinese Academy of Sciences, 20A Datun Road, Beijing 100012, China*
[2]*Jodrell Bank Centre for Astrophysics, University of Manchester, M13 9PL, UK*
[3]*Harvard-Smithsonian Center for Astrophysics 60 Garden Street, MS-51 Cambridge, MA, 02138, USA*

28 June 2011

ABSTRACT
Recent observations indicate that many if not all galaxies host massive central black holes (BHs). In this paper we explore the influence of supermassive binary black holes (SMBBHs) on the gravitational lensing properties. When lenses are modelled as singular isothermal ellipsoids, we show that a SMBBH system changes the critical curves and caustics when the system is very soft ($d \gtrsim 8.2$ kpc for a galaxy with velocity dispersion of $200\,\mathrm{km\,s^{-1}}$), while new critical curves can be created around the BHs when the separation of SMBBHs is not large $d < 8.2$ kpc). Each black hole can in principle gives rise to at least one additional image, which, if observed, provides evidence of black holes. By studying how SMBBHs affect the cumulative distribution of magnification for images created by black holes, we find that the cross section for such images (in the singular isothermal sphere model), whose magnifications are larger than 10^{-5}, is comparable to the cross section for producing multi-images in singular isothermal lenses. Such additional images may be detectable with high-resolution and large dynamic range maps of existing multiply-imaged systems from future facilities, such as the Square Kilometer Array (SKA). **smao: The probability of seeing these images is expectantly high if the fraction ($f_{\rm BH}$)of galaxies host binary black holes is sufficiently large ($f_{\rm BH} \gtrsim 0.1$).** We also study the effects of SMBBHs on the core images when galaxies have shallower central density profiles (modelled as non-singular isothermal ellipsoids). We find that the cross section of the usually faint core images is further suppressed by SMBBHs. Thus their presence should also be taken into account when one constrains the core radius from the lack of central images in gravitational lenses.

Key words: cosmology: theory – galaxy – gravitational lensing – binary black holes

1 INTRODUCTION

Recent observations suggest that many if not all nearby galaxies host massive central black holes. Empirical correlations have been discovered between the mass of the supermassive black holes (SMBHs) and various galaxy properties such as the bulge mass (Laor 2001; Marconi & Hunt 2003; Häring & Rix 2004; Novak et al. 2006; Graham & Driver 2007; Soker 2009), velocity dispersion (Ferrarese & Merritt 2000; Gebhardt et al. 2000; Tremaine et al. 2002; Nipoti et al. 2003; Robertson et al. 2006; Hu 2008; Feoli et al. 2011), luminosity (Magorrian et al. 1998; McLure & Dunlop 2001, 2002), and concentration (Graham et al. 2001). These correlations suggest that the growth of black hole is closely related to galaxy formation (Kauffmann & Haehnelt 2000; Monaco et al. 2000; Wyithe & Loeb 2002; Yu & Tremaine 2002; Volonteri et al. 2003; Di Matteo et al. 2003; Haiman et al. 2004; Ferrarese et al. 2006; Yu & Lu 2008; Bandara et al. 2009).

Gravitational lensing is an independent, mass-based method to probe SMBHs. The lensing effect of single SMBHs has been studied previously (Mao et al. 2001; Chen 2003a,b; Bowman et al. 2004; Rusin et al. 2005). Supermassive binary black holes are generated by merging of galaxies (Yu 2002; Berczik et al. 2006; Johansson et al. 2009), which is observed and predicted in the hierarchical structure formation theory. When two galaxies merge, their associated black holes will first decay through dynamical frictions. However, as the binary tightens and increases its velocity, dynamical friction becomes ineffective. The evolution of binary black holes may stall at $\mathrm{several\,pc} \sim \mathrm{several\,10pc}$ (Yu 2002). Some other (e.g., gas) processes bring the binary black holes closer until gravitational radiation rapidly merges the binary black holes into a single one. Currently, it is unknown how many binary black holes there are in the universe, and thus any probe of this population will provide additional constraints on the binary black hole formation and evolution.

The purpose of this paper is to study the effects of SMBBHs on lensing properties. We show that the presence of SMBBHs can not only disturb the critical curves of the primary lens galaxy but also create additional images. These additional images can potentially be observed by future radio facilities, such as the Square Kilo-

⋆ E-mail:uranus@bao.ac.cn
† E-mail:shude.mao@gmail.com

meter Array (SKA), which will provide high angular resolution and dynamic range. If lenses have shallow (non-singular) central profiles, central core images are predicted, but they may be destroyed by the presence of SMBBHs (Mao et al. 2001). We also examine this issue in some detail.

The outline of this paper is as follows. In section 2, we show the basic lensing model of a galaxy with SMBBHs, the non-singular isothermal ellipsoid which includes the singular isothermal ellipsoid as a special case. The classification of SMBBHs is also discussed in section 2. In section 3, we focus on critical curves and caustics of galaxy with SMBBHs. In section 4, we discuss the cross sections of BH-images above a certain magnification threshold and estimate the probability of these images being observed. In section 5, we study the influence of SMBBHs on the core images in non-singular isothermal lens models. Conclusions and discussions are given in section 6. Throughout this paper we assume a flat ΛCDM cosmology with $\Omega_{\rm m,0}=0.3$, $\Omega_{\Lambda,0}=0.7$ and Hubble constant $H_0=100\,h\ {\rm km\ s^{-1}\ Mpc^{-1}}$, $h=0.7$.

2 LENS MODEL OF GALAXY WITH SMBBHS

We model a lensing galaxy by an non-singular isothermal ellipsoid halo plus a SMBBHs. This model includes the singular isothermal ellipsoid model as a special case, which is not only analytically tractable but also consistent with models of individual lenses, lens satatistics, stellar dynamics and X-ray galaxies (Fabbiano 1989; Maoz & Rix 1993; Kochanek 1995, 1996; Grogin & Narayan 1996a,b; Rix et al. 1997). In other words, the core radii are expected to be small in elliptical galaxies (Wallington & Narayan 1993). In §2.1 we outline the lensing basics for a non-singular isothermal ellipsoid plus a SMBBHs. In §2.2, we focus on the classification of SMBBHs, which is an important factor for the influence of SMBBHs on gravitational lenses.

2.1 Non-singular isothermal Lens Model with SMBBHs

The dimensionless surface mass density distribution of non-singular isothermal ellipsoid is given by

$$\kappa=\frac{\Sigma}{\Sigma_{\rm cr}}=\frac{1}{2q}\frac{1}{\sqrt{x_1^2+x_2^2/q^2+r_{\rm c}^2}}, \tag{1}$$

where $r_{\rm c}$ is the core radius, q is the axis ratio and $\Sigma_{\rm cr}=c^2D_{\rm s}/(4\pi GD_{\rm d}D_{\rm ds})$ is the critical surface density, $D_{\rm d}$, $D_{\rm s}$ are angular diameter distances from the observer to the lens and source, respectively, and $D_{\rm ds}$ is the angular diameter distance from the lens to the source. All the lengths $(x_1,x_2,r_{\rm c})$ are expressed in units of the critical radius, $R_{\rm cr}$, which is also called the Einstein radius,

$$R_{\rm cr}=D_{\rm d}\theta_{\rm E,SIS},\qquad \theta_{\rm E,SIS}=4\pi\left(\frac{\sigma_{\rm v}}{c}\right)^2\frac{D_{\rm ds}}{D_{\rm s}}, \tag{2}$$

where the critical angle $\theta_{\rm E,SIS}$ is the angle subtended by the critical radius of the singular isothermal sphere lens on the sky ($\theta_{\rm E,SIS}\sim 0.2-3$ arcsec for typical lens galaxies), and the velocity dispersion $\sigma_{\rm v}$ is related to, but not necessarily identical to, the observable line-of sight velocity dispersion; we shall ignore this minor complication in our analysis and simply treat it as a parameter. For illustration purposes, we adopt a lens at redshift 0.5 and a source at redshift 2, velocity dispersion $\sigma_{\rm v}=200$ km/s and axis ratio $q=0.7$.

The lensing properties of the isothermal ellipsoid have been given by Kassiola & Kovner (1993); Kormann et al. (1994); Keeton & Kochanek (1998). The lens equation including a SMBBHs is given by

$$y_1=x_1-\frac{\sqrt{q}}{\sqrt{1-q^2}}\tan^{-1}\left(\frac{\sqrt{1-q^2}x_1}{\Phi+r_{\rm c}/q}\right)-m_1\left(\frac{x_1-u_1}{r_{\rm a}^2}\right)-m_2\left(\frac{x_1-v_1}{r_{\rm b}^2}\right) \tag{3}$$

$$y_2=x_2-\frac{\sqrt{q}}{\sqrt{1-q^2}}\tanh^{-1}\left(\frac{\sqrt{1-q^2}x_2}{\Phi+r_{\rm c}q}\right)-m_1\left(\frac{x_2-u_2}{r_{\rm a}^2}\right)-m_2\left(\frac{x_2-v_2}{r_{\rm b}^2}\right) \tag{4}$$

Where $\Phi^2=q^2x_1^2+x_2^2+r_{\rm c}^2$, and m_1, m_2 are the dimensionless mass of the two BHs respectively. We label the two BHs of SMBBHs as 'a', 'b'. $r_{\rm a}$, $r_{\rm b}$ are the dimensionless distances from the images to the black hole 'a', 'b', and (u_1,u_2), (v_1,v_2) are the coordinates of 'a' and 'b' on the lens plane

$$r=\sqrt{x_1^2+x_2^2}\,, \tag{5}$$

$$r_{\rm a}=\sqrt{(x_1-u_1)^2+(x_2-u_2)^2}\,, \tag{6}$$

$$r_{\rm b}=\sqrt{(x_1-v_1)^2+(x_2-v_2)^2}\,. \tag{7}$$

We also define

$$m=m_1+m_2, \tag{8}$$

$$m=\frac{M_{\rm bh}}{M_{\rm cr}},\qquad M_{\rm cr}=\frac{\pi\sigma_{\rm v}^2R_{\rm cr}}{G}, \tag{9}$$

with $M_{\rm bh}$ being the total mass of SMBBHs. Physically, $M_{\rm cr}$ is the mass of the galaxy contained within a cylinder with radius $R_{\rm cr}$ and hence m is the ratio of the total mass of SMBBHs to the mass of the galaxy in the inner parts (within $R_{\rm cr}$). We assume that the correlations of total mass of SMBBHs and the host galaxy are the same as a single BH's mass and its host galaxy. The black hole mass versus velocity dispersion correlation has been studied in detail by many people (Ferrarese & Merritt 2000; Gebhardt et al. 2000; Tremaine et al. 2002; Nipoti et al. 2003; Robertson et al. 2006; Hu 2008; Gültekin et al. 2009). The correlation is power law with a typical slope approximating to 4 (Tremaine et al. 2002; Gültekin et al. 2009) or 5 (Ferrarese & Merritt 2000). In our paper, we use the correlation of BHs' mass with velocity dispersion found by Gültekin et al. (2009)

$$M_{\rm bh}\approx 10^{8.23}M_\odot(\sigma_{\rm v}/200)^{3.96}, \tag{10}$$

for elliptical galaxies which dominate the lensing cross-sections. So the dimensionless total mass of SMBBHs is given by

$$m=2.5\times10^{-3}h\left(\frac{\sigma_{\rm v}}{200}\right)^{-0.04}. \tag{11}$$

Notice that m has little dependence on the velocity dispersion, although we caution that there is substantial scatter in this relation. The magnification (μ) is given by

$$\mu^{-1}=\frac{\partial y_1}{\partial x_1}\frac{\partial y_2}{\partial x_2}-\frac{\partial y_1}{\partial x_2}\frac{\partial y_2}{\partial x_1}. \tag{12}$$

The lens model has 10 degrees of freedom $(\vec{y},\vec{u},\vec{v},m_1/m_2,\sigma_{\rm v},q,r_{\rm c})$. even if we ignore the scatter the scatter the relation in m vs. $\sigma_{\rm v}$ (and set the core radius to zero). The parameter space is large, and thus in this paper we limit ourselves with typical illustrative, typical examples.

The lens equation has to be solved numerically. Through Eq. 12 above, we can use two ways to investigate the influence of SMBBHs on gravitational lenses. In general, there are several curves in the images plane along which the magnification is infinite ($\mu^{-1} = 0$). These are called critical curves, and they map to caustics in the source plane. Caustics mark discontinuities in the number of images, so in order to determine the number of images produced by a lens model. We can study the difference between the lens model with or without SMBBHs to obtain the effect of SMBBHs on gravitational lensing (see §3). We also calculate the cross section when the magnification of an image (generated by SMBBHs) is greater than a certain lower limit, e.g. $\mu > 10^{-5}$, which can be potentially observed. We study this in §4 and §5.

If we set the core size $r_{\rm c} = 0$, the non-singular isothermal model becomes a singular isothermal model, for which the influence of SMBBHs we will study in §3 and §4.

2.2 Classification of SMBBHs

We classify the SMBBHs by the separation of its two members. First, we calculate the condition that the rotation velocity of SMBBHs is equal to the velocity dispersion. In this case, the separation of SMBBHs is called critical separation ($d_{\rm cr}$),

$$\frac{GM_{\rm bh}}{4d_{\rm cr}} = v^2 \approx 2\sigma_{\rm v}^2, \tag{13}$$

$$d_{\rm cr} = \frac{GmM_{\rm cr}}{8\sigma_{\rm v}^2}, \tag{14}$$

The ratio of the critical separation to its host galaxy's Einstein Radius is

$$\frac{d_{\rm cr}}{R_{\rm cr}} = \frac{\pi m}{8} \approx 6.87\times10^{-4}\left(\frac{\sigma_{\rm v}}{200}\right)^{-0.04}. \tag{15}$$

We set the velocity dispersion $\sigma_{\rm v} = 200\,{\rm km\ s^{-1}}$ for definitiveness, the transition radius between soft and hard binary black holes $d_{\rm cr}$ can be estimated as

$$d_{\rm cr} \approx 3.53\,{\rm pc}, \tag{16}$$

which coincides with the most probable separation of SMBBHs (several pc $\sim$ several 10pc, Yu 2002). If the separation is much smaller than this radius, we call this SMBBHs 'hard', otherwise, 'soft'. Two other ratios are also relevant: the BH's Einstein radius to the host galaxy's Einstein radius. Assuming a lens redshift of 0.5 and a source redshift of 2, we have

$$\frac{\theta_{\rm E,BH}}{\theta_{\rm E,SIS}} = \sqrt{m} \approx 4.18\times10^{-2}\left(\frac{\sigma_{\rm v}}{200}\right)^{-0.02}, \tag{17}$$

and the critical separation to the BH's Einstein radius:

$$\frac{\theta_{\rm BH}}{\theta_{\rm E,BH}} = \frac{\pi\sqrt{m}}{8} \approx 1.64\times10^{-2}\left(\frac{\sigma_{\rm v}}{200}\right)^{-0.02}. \tag{18}$$

Both quantities are a few percent.

3 CRITICAL CURVES AND CAUSTICS OF SINGULAR ISOTHERMAL ELLIPSOID LENS WITH SMBBHS

As we discussed in the previous section, critical curves represent the positions of images of infinite magnification, while caustics mark discontinuities in the number of images. In this section, we study how the SMBBHs affect the critical curves and caustics of gravitational lens for a singular isothermal lenses (i.e., $r_{\rm c} = 0$).

We show the critical curves and caustics of singular isothermal model with central SMBBHs with different separations in Fig. 1. As can be seen, there are some critical curves near the BHs (which for convenience we will call them black hole critical curves) when the separation of SMBBHs is non-zero and $d \leq 1.6$ **smao: which is about** 8.2 **kpc, here** d **is the separation of SMBBHs which is in units of Einstein radius of singular isothermal sphere halo**. The black hole critical curves are a single continuous curve when the separation is very small ($d \lesssim 0.05$). They become several disjoint curves when the separation becomes larger ($d \geq 0.05$). These behaviours are also reflected in the caustics. When the separation becomes even larger ($d \approx 0.5$) the black hole critical curves become smaller and smaller. However, when the separation of SMBBHs becomes very large, **smao: e.g. the separation is larger than** 1.6 $(8.2\ {\rm kpc})$, the critical curves of the primary lens can be disturbed by BHs **smao: and the black hole critical curves are merging in to the primary critical curves**, so we have peculiar caustics as shown in the right bottom panel in Fig. 1. Such large separations are not expected to be common in the SMBBHs formation **smao: (Yu 2002; Colpi & Dotti 2009)**.

We also show some examples of images in Fig. 1, we can see that each black hole of SMBBHs can generate BH-images near itself, and if the source is located in a special position, e.g. near the psuedo-caustics, there will be multi BH-images for one black hole and there is at least one image of which the magnification is greater than 10^{-5}. When the separation of the SMBBHs is zero (single supermassive black hole), the source outside the primary critical curves, and there is a BH-image near the SMBBHs, which is shown in panel (a). As is well known, for a singular isothermal ellipsoid lens, if the source is located outside the primary critical curve (i.e. pseudo-caustics), there will be no multi-images, so this central image must be generated by the central SMBH. In panel (b) and (c), when the separations are not very large the black hole critical curve is continuous, and we find there are 3 BH-images for these two cases. In panel (d), there separation is larger than 0.05 and the black hole critical curves become disjoint, the black hole close to the source can generate a BH-images, the black hole that is further away from the source generates 3 BH-images while there is also another usual image around the position $(x = -0.081, y = -0.051)$. For panels (e), (f), and (g), the cases are similar, BH-images are generated close to each BH, and there is also an SIE-image close to the primary critical curves. The most unusual case is shown in the bottom right panel, the separation is such that the black holes distort the primary critical curves, 8 images are created in total, including 4 BH-images. Some of these BH-images are bright ($|\mu| > 0.425$) enough to be detected, but the probability may be low because a large separation (11.6 kpc for our illustrative example) is required, and most black holes may not be at such large distances.

In the other extreme, very hard SMBBHs (i.e., with very small separations, $d \lesssim 10^{-6}$ in the Einstein radius) affect the critical curves of singular isothermal halos. In principle, the rapid rotation may lead to variations in the magnification. However, for this to be observable, its timescale needs to be relatively short, $T/4 \lesssim 10\,{\rm yr}$, where the period $T = (d^3/(GM_{\rm bh}))^{1/2}$. This requires a separation for $d \lesssim 0.04$pc for a total black hole mass of $1.7\times10^8 M_\odot$ corresponding to $\sigma_{\rm v} = 200\,{\rm km/s}$. This separation is much smaller than $d_{\rm cr}$, and thus the binary black holes will essentially appear as a single one for lensing purposes. We conclude that in general the binary rotation effect will be difficult to detect using current or even future facilities.

The above discussion shows that the effects of SMBBHs on critical curves and caustics of singular isothermal model is sen-

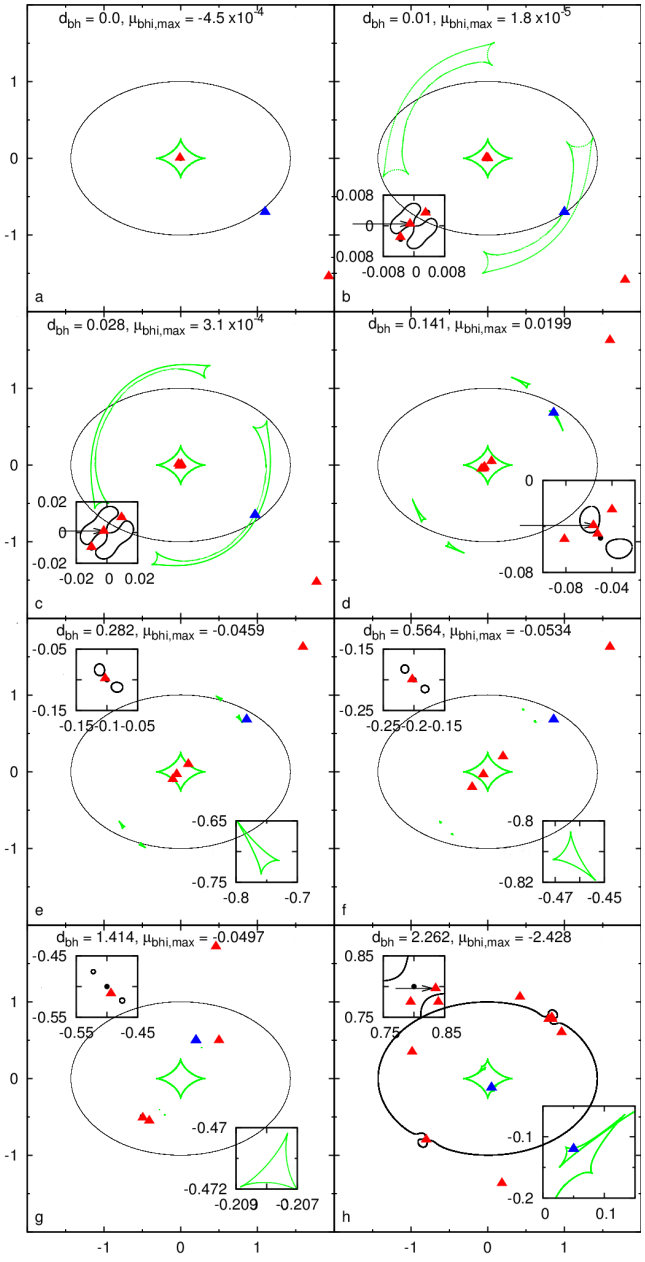

Figure 1. Critical curves and caustics for the case of a central SMBBHs in a singular isothermal galaxy, and also examples of images. The mass ratio for the binary system is $m_1/m_2 = 1$, and the separation ($d_{\rm bh}$) is indicated in each panel. $d_{\rm bh}$ is in units of $r_{\rm E,SIS}$, the Einstein radius of the singular isothermal sphere model. The black curves show the critical curves, while the green curves show the caustics, blue triangles show the sources' positions and red triangles show the images' positions. We also plot SMBBHs' positions in these panels (black points). All SMBBHs cases have $m = 2.5\times10^{-3}h$, and the galaxy is singular isothermal with velocity dispersion $\sigma_{\rm v} = 200$ km s^{-1} and axis ratio $q = 0.7$. The highest black hole image magnification is labelled for each case.

sitive to the distance from the members to the center of the host galaxy. When BHs are near the center of galaxy, the black hole critical curves, which are generated by BHs, can map into remarkable caustics. It means that the cross section of extra BH-images, which will be discussed in detail in §4, is larger when the BHs is near the center of the halo.

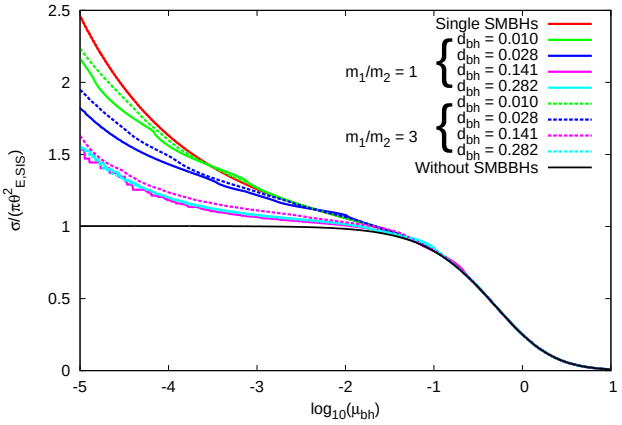

Figure 2. Cumulative distribution functions for the magnification of all images in the SIE-SMBBHs lens model. These color curves show SMBBHs cases with different separations which are indicated in the top-right of the figure. The black solid curve shows the cumulative distribution function for the magnification of a singular isothermal lens model (without BHs). All SMBBHs cases have a total mass of $m = 2.5 \times 10^{-3}h$. The mass ratios are $m_1/m_2 = 1$ (solid curves) and $m_1/m_2 = 3$ (dash cures). The galaxies are modelled as singular isothermal models with velocity dispersion $\sigma_{\rm v} = 200$ km s^{-1}, and axis ratio $q = 0.7$.

4 CROSS SECTIONS AND PROBABILITY

In this section, we investigate the influence of SMBBHs on cross sections of BH-images of singular isothermal ellipsoid halos, whose magnifications are greater than $10^{-3}, 10^{-4}$ and 10^{-5} respectively, which we will use to estimate the observational probability of BH-images which are generated by a galaxy with SMBBHs lens under different lower limit of magnifications. In addition, the probability that both two BHs can generate BH-images with magnifications greater than $10^{-3}, 10^{-4}$ and 10^{-5} will be studied.

4.1 Cross Sections

Fig. 2 shows the cumulative cross sections distribution function, where we plot two mass ratios of SMBBHs are $m_1/m_2 = 1$ and $m_1/m_2 = 3$. In each case there are 4 different separations. The heavy black line is the cumulative cross section distribution function of singular isothermal model, the color lines, show the cumulative cross section distribution function of SIE-SMBBHs with different separations of SMBBHs. Solid color lines show the cases that the SMBBHS are equal-mass except that the solid red line show the cases that the separation of SMBBHs is 0, dashed color line show the cases that the mass ratio of SMBBHs is $m_1/m_2 = 3$. So the value that color lines in excess of the heavy solid line at the same magnification is the cross section of images which are generated by BHs. The cross sections will become smaller when the separation becomes larger at small magnification. Non-equal mass SMBBHs will give larger cross sections than equal mass SMBBHs when the separations are not so large, but this difference becomes negligible when the separation becomes larger since the cross-section converges, because the SMBBHs can be considered as two separate single BHs and their cross-sections simply add.

We give the relation of cross-sections and the SMBBHs' separations when the magnification is greater than $10^{-3}, 10^{-4}$ and 10^{-5} for a singular isothermal model respectively. As shown in

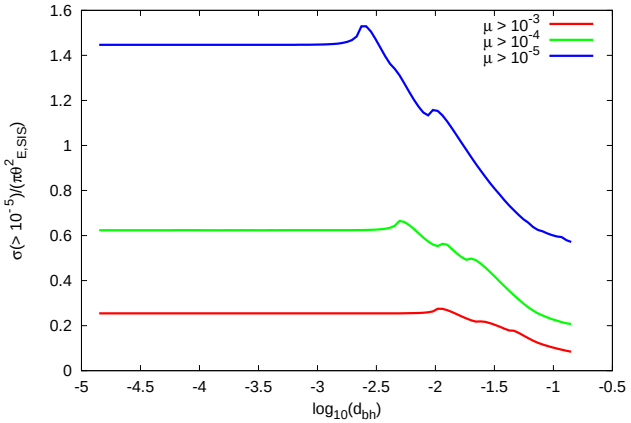

Figure 3. Cross-section of BH-images of SIE-SMBBHs model as a function of separation $d_{\rm bh}$ of SMBBHs with different lower limits of magnification. The red, green and blue curves correspond to a lower limit of $10^{-3}, 10^{-4}$ and 10^{-5} respectively. All SMBBHs cases have $m = 2.5 \times 10^{-3}h$, $m_1/m_2 = 1$. Both galaxies are singular isothermal ellipsoids with velocity dispersion $\sigma_{\rm v} = 200$ km s^{-1}, and axis ratio $q = 0.7$.

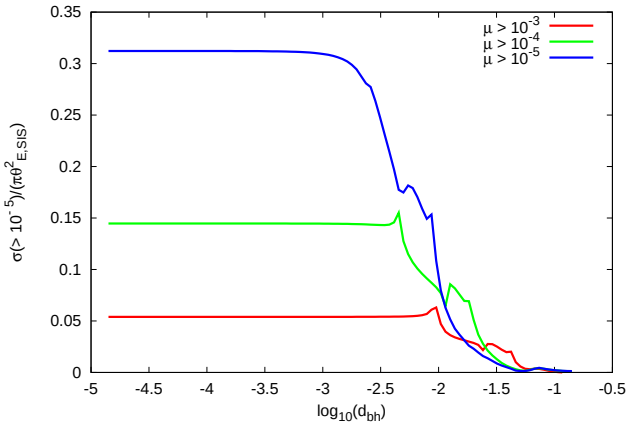

Figure 4. Similar to Fig. 3, except that cross section is for the case when both BHs create BH-images with magnification greater than three lower limits as in Fig. 3. All SMBBHs cases have $m = 2.5 \times 10^{-3}h$, and the mass ratio $m_1/m_2 = 1$. Both galaxies are modelled as singular isothermal ellipsoids with velocity dispersion $\sigma_{\rm v} = 200$ km s^{-1} and axis ratio $q = 0.7$.

Fig 3, the higher the lower limit of magnification, the larger the cross section of the BH-images. The peak of the curve will move to the large separation end and vanish.

Fig. 4 illustrates the cross-section that we can detect 2 BH-images, which are generated by both members of the SMBBHs respectively. As shown in Fig. 4, only when the separation is small enough, **smao: then** both-BH-images can be generated, and the higher the lower limit of the magnification is, the larger the cross section of BH-images is.

5 SUPPRESSION OF CORE IMAGES IN A NON-SINGULAR ISOTHERMAL GALAXY WITH SMBBHS

In this section, we investigate the cross section distribution function of core images of non-singular isothermal ellipsoid (NIE) lens model. As is well known, non-singular isothermal model can generate a faint core images, and the magnification and position of the core image are sensitive to the core size of the halo, so one can constrain the core size of non-singular isothermal halo through the probability of core images in the lens survey, but we show below, as in the case of a single central black hole, the presence of SMBHs (SMBBHs) can also suppress the probability of core images.

As previously, we set the velocity dispersion $\sigma_{\rm v} = 200$ km s^{-1}, axis ratio $q = 0.7$ and core size $r_{\rm c} = 0.05$. Fig. 5 shows the cumulative distribution function for the magnification of core images ($\mu_{\rm core}$). SMBBHs suppress the faint end of the distribution, leaving the bright end largely unaffected. A smaller separation will suppress the faint end of the distribution more effectively than a larger separation. For $d_{\rm bh} \lesssim 0.04$, the suppression is of the order of 12%, and for $d_{\rm bh} \sim 0.20$ the suppression is of the order of 3%. Non-equal mass SMBBHs lead to smaller variations between different separations than equal mass SMBBHs. For example, for $d_{\rm bh} \sim 0.20$ with $m_1/m_2 = 3$, the suppression is of the order of 7%, Fig. 6 shows the cumulative distribution function for the magnification of core images in non-singular isothermal lens with more massive SMBBHs, whose total dimensionless mass is 0.01. We can see that the cross section of core images will be suppressed more at the faint end of the distribution because of the more massive SMBBHs. To summarize, there is some difference in the core images between single and double black holes, which will lead to slightly more uncertainty in the constraints on the core size.

6 DISCUSSION AND CONCLUSIONS

In this paper, we have studied the lensing configuration due to supermassive binary black holes (SMBBHs). We have shown typical examples of critical curves, caustics, and image configurations. Similar to a single black hole, SMBBHs can create additional images close to them.

As we discussed above, for singular isothermal lenses, the cross section will be larger when BHs move to the center of the galaxy. The cross section of singular isothermal lens, when the lower limit are greater than 10^{-5}, is comparable with the multi-images cross section of singular isothermal sphere lens model. So we can estimate the probability as $P_{\rm BH}(>\mu) \approx \mathcal{R}_{\rm BH}(>\mu)\, f_{\rm BH}$. Here, $\mathcal{R}_{\rm BH}$ is the ratio of the cross section of BH-images to the cross section of multi-images in singular isothermal sphere lens, **smao: and $f_{\rm BH}$ is the fraction of galaxies which has SMBBHs.**

The values of $\mathcal{R}_{\rm BH}$ can be read off from Fig. 2 and Fig. 3. Thus, the observational probability of the BH-images in a multi-images lens system, whose magnification are greater than $10^{-3}, 10^{-4}$ and 10^{-5}, are about $0.2 f_{\rm BH}$, $0.6 f_{\rm BH}$ and $1.4 f_{\rm BH}$ respectively. and the probability of the case that both BHs can generate one BH-image at least, whose magnification are greater than $10^{-3}, 10^{-4}$ and 10^{-5}, are about $5 \times 10^{-2} f_{\rm BH}$, $1.5 \times 10^{-1} f_{\rm BH}$ and $3 \times 10^{-1} f_{\rm BH}$ respectively. We can see clearly that the probability are sensitive to the fraction of galaxies which have SMBBHs, so if $f_{\rm BH}$ is sufficiently large, the probability is observable. We also have to mind the separations of the additional BH-images to approximate the observability of BH-images. It is shown in Fig. 1, the

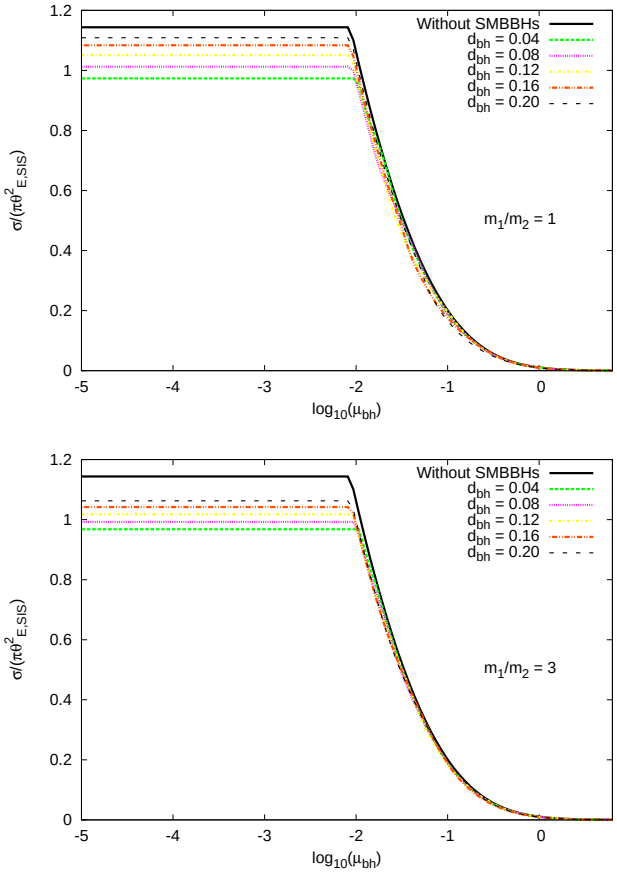

Figure 5. Cumulative distribution functions for the magnification of core-images in the non-singular isothermal halo with SMBBHs lens. The heavy curves show the case without BHs. The light curves show SMBBHs cases with separations $d_{\rm cr} = 0.04, 0.08, ..., 0.20$. All SMBBHs cases have $m = 2.5 \times 10^{-3}h$, and (Top) $m_1/m_2 = 1$, (Bottom) $m_1/m_2 = 3$. Both galaxies are modelled as non-singular isothermal ellipsoids with core radius $r_{\rm c} = 0.05$, velocity dispersion $\sigma_{\rm v} = 200$ km s^{-1} and axis ratio $q = 0.7$.

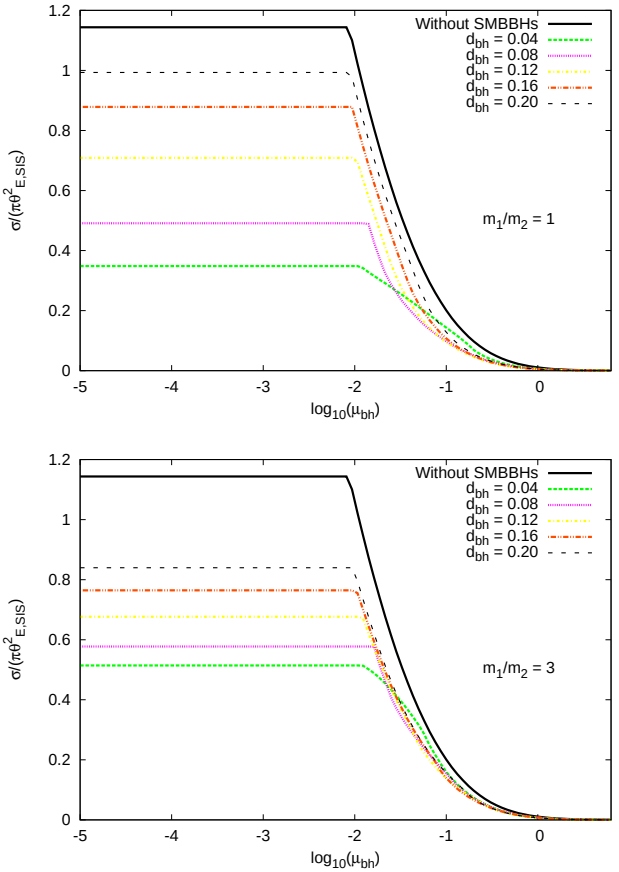

Figure 6. Similar to Fig. 5, except that the total dimensionless mass of SMBBHs is $m = 0.01$.

BH-images are very near to the BHs, so we can consider the separations of BHs as the separations of the BH-images, of which the most probable separations is $\sim 10^{-4}$ in units of $R_{\rm E,SIS}$. So the resolution should be better than 10^{-4} arcsec **smao: which is already touched by recent facilities**. **smao: On the other hand, we need very high large dynamic range to detect the BH-images when the magnifications of BH-images are small, e.g. when the magnification of BH-image is 10^{-3}, the dynamic ranges of the observer has to be greater than $10^{-3}/\mu_{\rm Brightest}$, here $\mu_{\rm Brightest}$ is the magnification of the brightest image in SIE-SMBBHs lens, and $\mu_{\rm Brightest}$ is about $1 \sim 10$ except that the brightest image locate near the critical curves, so if we want to detect a BH-image whose magnification is 10^{-3}, as a conservative estimate, the dynamic ranges of the observer needs to be 10^{-4}.**

Of course, there are several factors can distort the cross section and the probability in the singular isothermal model: axis ratio, orientations of axis of SMBBHs and mass ratio of SMBBHs. In our work, we have calculated these cases and find no significant effects with different axis ratios, orientations of axis of SMBBHs andmass ratios of SMBBHs. It is interesting to speculate what we can learn if we do observe If we get 2 BH-images case of singular isothermal lens with SMBBHs, we have 4 additional constraints, and we have 5 parameters because $\vec{x}$, q, $r_{\rm c}$, $\sigma_{\rm v}$ can be got from observations, so we can constrain the projected information of this SMBBHs in principle. However, if the lens is non-singular isothermal ellipsoid, the number of parameters will exceed the number of additional constraints, and so we will not be able to derive the parameters uniquely. including the core size and the parameters of SMBBHs, We find that the presence of SMBBHs can suppress the faint end of the cumulative distribution for the magnification of core images, and leave the bright end largely unaffected, and so their effect, will needs to be accounted for in the constraint on the central mass profiles (e.g., core radius).

To summarize, gravitational lensing can be in principle used to detect SMBHs in galaxies through the extra images they create. Unfortunately, these images are usually very faint, and pose challenges for detection using current instruments. However, a much larger sample of lenses will be available in future surveys such as LSST ([1]), and a new generation of instruments, such as the Square Kilometer Array (SKA), will become available. SKA will provide very high-contrast ($\gtrsim 10^6$) and very high-resolution ($\lesssim 10^{-4}$ arcsec) imaging capabilities, we remain cautiously optimistic that such black holes can be independently discovered through careful observations of multiply-image systems.

[1] www.lsst.org

ACKNOWLEDGMENTS

We would like to thank Chuck Keeton, Youjun Lu, Xinzhong Er and Dandan Xu for advice and useful discussions on the topic.

REFERENCES

Bandara K., Crampton D., Simard L., 2009, ApJ, 704, 1135
Berczik P., Merritt D., Spurzem R., Bischof H.-P., 2006, ApJ, 642, L21
Bowman J. D., Hewitt J. N., Kiger J. R., 2004, ApJ, 617, 81
Chen D., 2003a, ApJ, 587, L55
Chen D., 2003b, A&A, 397, 415
Colpi M., Dotti M., 2009, ArXiv e-prints
Di Matteo T., Croft R. A. C., Springel V., Hernquist L., 2003, ApJ, 593, 56
Fabbiano G., 1989, ARA&A, 27, 87
Feoli A., Mancini L., Marulli F., van den Bergh S., 2011, General Relativity and Gravitation, 43, 1007
Ferrarese L., Côté P., Dalla Bontà E., Peng E. W., Merritt D., Jordán A., Blakeslee J. P., Haşegan M., Mei S., Piatek S., Tonry J. L., West M. J., 2006, ApJ, 644, L21
Ferrarese L., Merritt D., 2000, ApJ, 539, L9
Gebhardt K., Bender R., Bower G., Dressler A., Faber S. M., Filippenko A. V., Green R., Grillmair C., Ho L. C., Kormendy J., Lauer T. R., Magorrian J., Pinkney J., Richstone D., Tremaine S., 2000, ApJ, 539, L13
Graham A. W., Driver S. P., 2007, ApJ, 655, 77
Graham A. W., Erwin P., Caon N., Trujillo I., 2001, ApJ, 563, L11
Grogin N. A., Narayan R., 1996a, ApJ, 464, 92
Grogin N. A., Narayan R., 1996b, ApJ, 473, 570
Gültekin K., Richstone D. O., Gebhardt K., Lauer T. R., Tremaine S., Aller M. C., Bender R., Dressler A., Faber S. M., Filippenko A. V., Green R., Ho L. C., Kormendy J., Magorrian J., Pinkney J., Siopis C., 2009, ApJ, 698, 198
Haiman Z., Ciotti L., Ostriker J. P., 2004, ApJ, 606, 763
Häring N., Rix H.-W., 2004, ApJ, 604, L89
Hu J., 2008, MNRAS, 386, 2242
Johansson P. H., Burkert A., Naab T., 2009, ApJ, 707, L184
Kassiola A., Kovner I., 1993, ApJ, 417, 450
Kauffmann G., Haehnelt M., 2000, MNRAS, 311, 576
Keeton C. R., Kochanek C. S., 1998, ApJ, 495, 157
Kochanek C. S., 1995, ApJ, 445, 559
Kochanek C. S., 1996, ApJ, 466, 638
Kormann R., Schneider P., Bartelmann M., 1994, A&A, 284, 285
Laor A., 2001, ApJ, 553, 677
Magorrian J., Tremaine S., Richstone D., Bender R., Bower G., Dressler A., Faber S. M., Gebhardt K., Green R., Grillmair C., Kormendy J., Lauer T., 1998, AJ, 115, 2285
Mao S., Witt H. J., Koopmans L. V. E., 2001, MNRAS, 323, 301
Maoz D., Rix H., 1993, ApJ, 416, 425
Marconi A., Hunt L. K., 2003, ApJ, 589, L21
McLure R. J., Dunlop J. S., 2001, MNRAS, 327, 199
McLure R. J., Dunlop J. S., 2002, MNRAS, 331, 795
Monaco P., Salucci P., Danese L., 2000, MNRAS, 311, 279
Nipoti C., Londrillo P., Ciotti L., 2003, MNRAS, 342, 501
Novak G. S., Faber S. M., Dekel A., 2006, ApJ, 637, 96
Rix H., de Zeeuw P. T., Cretton N., van der Marel R. P., Carollo C. M., 1997, ApJ, 488, 702
Robertson B., Hernquist L., Cox T. J., Di Matteo T., Hopkins P. F., Martini P., Springel V., 2006, ApJ, 641, 90
Rusin D., Keeton C. R., Winn J. N., 2005, ApJ, 627, L93
Soker N., 2009, MNRAS, 398, L41
Tremaine S., Gebhardt K., Bender R., Bower G., Dressler A., Faber S. M., Filippenko A. V., Green R., Grillmair C., Ho L. C., Kormendy J., Lauer T. R., Magorrian J., Pinkney J., Richstone D., 2002, ApJ, 574, 740
Volonteri M., Haardt F., Madau P., 2003, ApJ, 582, 559
Wallington S., Narayan R., 1993, ApJ, 403, 517
Wyithe J. S. B., Loeb A., 2002, ApJ, 581, 886
Yu Q., 2002, MNRAS, 331, 935
Yu Q., Lu Y., 2008, ApJ, 689, 732
Yu Q., Tremaine S., 2002, MNRAS, 335, 965